Inorg. Chem. **2003**, *42*, 6183–6193

Core-Modified Porphyrin Incorporating a Phenolate Donor. Characterization of Pd(II), Ni(II), Zn(II), Cd(II), and Fe(III) Complexes

Marcin Stępień and Lechosław Latos-Grażyński*

Department of Chemistry, University of Wrocław,14 F. Joliot-Curie St., Wrocław 50 383, Poland

Received May 14, 2003

Coordinating properties of acetoxybenziporphyrin, (TPBPOAc)H, have been investigated for a number of metal ions. Insertion of Ni, Pd, and Fe results in the cleavage of the acetoxy group leading to complexes (TPBPO)Ni^{II}, (TPBPO)Pd^{II}, and (TPBPO)$Fe^{III}X$ containing a M–O bond. No cleavage is observed with Zn(II) and Cd(II), which form complexes (TPBPOAc)$M^{II}Cl$, where M = Zn, Cd. (TPBPO)Ni^{II} can also be obtained from the dication of hydroxybenziporphyrin, $[(TPBPOH)H_3]Cl_2$, which is prepared by acid hydrolysis of the acetoxy compound. The diamagnetic (TPBPO)Ni^{II} can be transformed into the paramagnetic (TPBPOAc)$Ni^{II}Cl$ in a reaction with acetyl chloride. X-ray structures have been determined for (TPBPO)Pd^{II} and (TPBPOAc)$Zn^{II}Cl$. In the palladium species, the phenolate moiety forms a strong bond to the Pd ion and an unusual interaction geometry is observed, enforced by the macrocyclic environment. Association of a TFA molecule to the phenolic oxygen does not cause significant structural changes in the (TPBPO)Pd^{II} molecule. In (TPBPOAc)$Zn^{II}Cl$, the metal ion weakly interacts with the phenolic fragment. The paramagnetic Fe(III) complexes, (TPBPO)$Fe^{III}X$, have been investigated with ^1H NMR spectroscopy. The observed spectral patterns are consistent with the presence of a high-spin Fe(III) center and π delocalization of spin density onto the phenoxide fragment. Each of the compounds (TPBPO)$Fe^{III}X$ exists in solution as a mixture of two isomers, which for X = I are shown to remain in a temperature-dependent equilibrium. The observed isomerism results from two nonequivalent orientations of the axial halide with respect to the puckered macrocyclic ring.

Introduction

One of the primary goals driving the search for new core-modified porphyrins is the synthesis of macrocycles that provide a favorable environment to stabilize less-common coordination modes between metal ions and a donor of choice.[1] This goal is well exemplified by the coordination properties of carbaporphyrinoids, a novel class of macrocycles capable of generating rich organometallic chemistry.[1−5] Their construction formally requires a modification of the porphyrin skeleton that would provide a CH unit in place of one of the nitrogens. It is effected by replacing one pyrrole ring by an appropriate moiety, such as *m*-phenylene,[6,7] *p*-phenylene,[8] semiquinone,[9−11] cycloheptatriene,[12,13] indene,[12,14] azulene,[15−18] cyclopentadiene,[19] or 2,4-linked thiophene.[20]

Some of the resultant molecules can be derivatized by exploiting their inherent reactivity. When the reaction affects the exterior of the macrocycle, the (N,N,N,C) coordination

* Author to whom correspondence should be addressed. E-mail: llg@wchuwr.chem.uni.wroc.pl.

(1) Latos-Grażyński, L. Core Modified Heteroanalogues of Porphyrins and Metalloporphyrins. *The Porphyrin Handbook*; Kadish, K. M., Smith, K. M., Guilard, R., Eds.; Academic Press: New York, 2000; Vol. 2, Chapter 14, pp 361−416.
(2) Chmielewski, P. J.; Latos-Grażyński, L.; Rachlewicz, K.; Głowiak, T. *Angew. Chem., Int. Ed. Engl.* **1994**, *33*, 779.
(3) Furuta, H.; Asano, T.; Ogawa, T. *J. Am. Chem. Soc.* **1994**, *116*, 767.
(4) Lash, T. D. *Synlett* **1999**, 279.
(5) Furuta, H.; Maeda, H.; Osuka, A. *Chem. Commun.* **2002**, 1795.
(6) Berlin, K.; Breitmaier, E. *Angew. Chem., Int. Ed. Engl.* **1994**, *33*, 1246.
(7) Stępień, M.; Latos-Grażyński, L. *Chem.−Eur. J.* **2001**, *7*, 5113.
(8) Stępień, M.; Latos-Grażyński, L. *J. Am. Chem. Soc.* **2002**, *124*, 3838.
(9) Lash, T. D. *Angew. Chem., Int. Ed. Engl.* **1995**, *34*, 2533.
(10) Lash, T. D.; Chaney, S. T.; Richter, D. T. *J. Org. Chem.* **1998**, *63*, 9076.
(11) Liu, D.; Lash, T. D. *Chem. Commun.* **2002**, 2426.
(12) Berlin, K.; Steinbeck, C.; Breitmaier, E. *Synthesis* **1996**, 336.
(13) Lash, T. D.; Chaney, S. T. *Tetrahedron Lett.* **1996**, *37*, 8825.
(14) Lash, T. D.; Hayes, M. J. *Angew. Chem., Int. Ed. Engl.* **1997**, *36*, 840.
(15) Lash, T. D.; Chaney, S. T. *Angew. Chem., Int. Ed. Engl.* **1997**, *36*, 839.
(16) Lash, T. D. *Chem. Commun.* **1998**, 1683.
(17) Venkatraman, S.; Anand, V. G.; PrabhuRaja, H.; Rath, H.; Sankar, J.; Chandrashekar, T. K.; Teng, W.; Ruhlandt-Senge, K. *Chem. Commun.* **2002**, 1660.
(18) Graham, S. R.; Colby, D. A.; Lash, T. D. *Angew. Chem., Int. Ed.* **2002**, *41*, 1371.
(19) Berlin, K. *Angew. Chem., Int. Ed. Engl.* **1996**, *35*, 1820.
(20) Sprutta, N.; Latos-Grażyński, L. *Tetrahedron Lett.* **1999**, *40*, 8457.

10.1021/ic0345121 CCC: $25.00
Published on Web 09/09/2003

Scheme 1

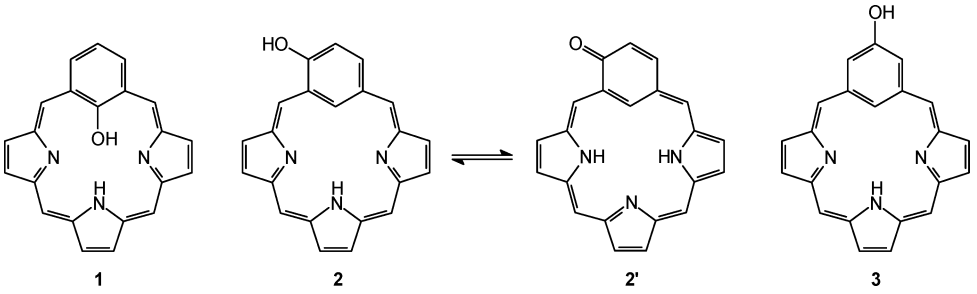

1 **2** **2'** **3**

core of a carbaporphyrinoid is preserved although the structure may otherwise be deeply altered.[16,20−26] If, however, the substitution takes place at the internal carbon, the coordinating properties of the molecule are directly affected.[27] In some cases, a potential donor atom is actually introduced, leading to a new type of porphyrin-related ligand.[28,29] The metal−donor bond can be firmly held in the cavity of such a ligand so that possible dissociation will be impaired.

This approach was explored for regular porphyrins, as examplified by the coordination of porphyrin *N*-oxide,[30−33] insertion of vinylidene carbene into the Fe−N nitrogen bond of iron porphyrin,[33−35] or isolation of the bridging methylene complex Ru(OEP−N-μ-CH_2−)(CH_3).[36] In those compounds, oxygen and carbon donors were introduced into the porphyrin core leading to peculiar coordination environments, (N,N,N,O-(N)) and (N,N,N,C(N)).

A natural modification of this type that can be applied to *m*-benziporphyrin is the introduction of a phenolate donor to the coordination core. The pertinent compound, 22-hydroxybenziporphyrin (**1**) is one of three isomeric benziporphyrins containing a phenolic function, the other two being 2-hydroxy- and 3-hydroxybenziporphyrin (**2** and **3**, respectively). These species correspond to the three distinct ways of incorporating a phenol moiety into the porphyrin macrocycle. In **2** and **3**, the (N,N,N,C) coordination core is retained, while in **1** it becomes (N,N,N,O(C)). Of the three

Scheme 2

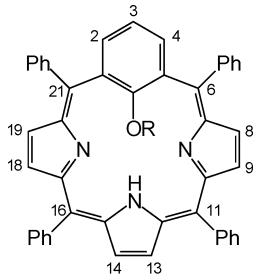

4 (R = Ac)
5 (R = H)

isomers, only the alkyl-substituted form of **2** was reported until now.[9] It exists preferentially as the 18-electron aromatic keto tautomer **2′** and, hence, was called 2-oxybenziporphyrin. Such an aromatic tautomer is not available for **1** or **3**. A disubstituted compound, 2-oxy-4-hydroxybenziporphyrin, was reported subsequently.[37] 8,19-Dimethyl-9,13,14,18-tetraethyl-2-oxybenziporphyrin coordinated palladium(II) to form the four-coordinate anionic complex $[(OBP)Pd^{II}]^-$.[38] The NMR data provided evidence for the retention of macrocyclic aromaticity and coordination via a carbon σ-donor. The phenolic structure of type **2** could be restored by protonation or alkylation of the external oxygen.

In the course of our studies on coordinating properties of 6,11,16,21-tetraphenyl-*m*-benziporphyrin, we found that in the reaction with silver(I) acetate, the macrocycle was selectively acetoxylated at the internal carbon atom yielding 22-acetoxy-6,11,16,21-tetraphenyl-*m*-benziporphyrin (**4**).[7] X-ray structural analysis of **4** confirmed that the benzene ring built into the framework of acetoxy-*m*-benziporphyrin completely blocks macrocyclic delocalization while retaining the unperturbed [6]annulene aromaticity, similar to the substrate *m*-benziporphyrin.

Compound **4** can be viewed as an O-protected 22-hydroxy-6,11,16,21-tetraphenyl-*m*-benziporphyrin (**5**), corresponding to the phenolic structure **1**. Symbols (TPBPOAc)H and (TPBPOH)H will be adopted for **4** and **5**, respectively, to denote the internal substitution. Deprotection of the OH group in **4** can, in principle, be carried out by either acid hydrolysis or metal insertion. In the latter case, **4** would lead directly to complexes of **5**, thus obviating the hydrolysis step. Cleavage of the ester function may depend on reaction

(21) Chmielewski, P. J.; Latos-Grażyński, L. *J. Chem. Soc., Perkin Trans. 2* **1995**, 503.
(22) Chmielewski, P. J.; Latos-Grażyński, L.; Głowiak, T. *J. Am. Chem. Soc.* **1996**, *118*, 5690.
(23) Schmidt, I.; Chmielewski, P. J. *Tetrahedron Lett.* **2001**, *42*, 1151.
(24) Schmidt, I.; Chmielewski, P. J.; Ciunik, Z. *J. Org. Chem.* **2002**, *67*, 8917.
(25) Furuta, H.; Maeda, H.; Osuka, A.; Yasutake, M.; Shinmyozu, T.; Ishikawa, Y. *Chem. Commun.* **2000**, 1143.
(26) Furuta, H.; Ishizuka, T.; Osuka, A.; Ogawa, T. *J. Am. Chem. Soc.* **1999**, *121*, 2945.
(27) Ishikawa, Y.; Yoshida, I.; Akaiwa, K.; Koguchi, E.; Sasaki, T.; Furuta, H. *Chem. Lett.* **1997**, 453.
(28) Hayes, M. J.; Spence, J. D.; Lash, T. D. *Chem. Commun.* **1998**, 2409.
(29) Hung, C.-H.; Chen, W.-C.; Lee, G.-H.; Peng, S.-M. *Chem. Commun.* **2002**, 1516.
(30) Balch, A. L.; Chan, Y. W.; Olmstead, M. M. *J. Am. Chem. Soc.* **1986**, *107*, 6510.
(31) Groves, J. T.; Watanabe, Y. *J. Am. Chem. Soc.* **1988**, *110*, 8443.
(32) Tsurumaki, H.; Watanabe, Y.; Morishima, I. *J. Am. Chem. Soc.* **1993**, *115*, 11784.
(33) Rachlewicz, K.; Latos-Grażyński, L. *Inorg. Chem.* **1996**, *35*, 1136.
(34) Chevrier, B.; Weiss, R.; Chottard, J.-C.; Lange, M.; Mansuy, D. *J. Am. Chem. Soc.* **1981**, *103*, 2899.
(35) Latos-Grażyński, L.; Cheng, R.-J.; La Mar, G. N.; Balch, A. L. *J. Am. Chem. Soc.* **1981**, *103*, 4270.
(36) Seyler, J. W.; Safford, L. K.; Fanwick, P. E.; Leidner, C. R. *Inorg. Chem.* **1992**, *31*, 1545.
(37) Richter, D. T.; Lash, T. D. *Tetrahedron* **2001**, *57*, 3657.
(38) Stępień, M.; Latos-Grażyński, L.; Lash, T. D.; Szterenberg, L. *Inorg. Chem.* **2001**, *40*, 6892.

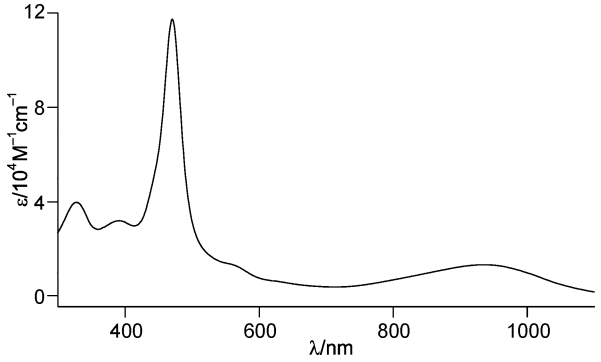

Figure 1. Electronic spectrum of $[\mathbf{5}-H_2]Cl_2$ (CH_2Cl_2, 298 K).

conditions and the choice of metal, making acetoxybenziporphyrin a versatile ligand.

Removal of the acetyl group should enable phenoxide coordination supported in a peculiar arrangement by the porphyrinoid ring, similar to the complexes of other macrocyclic[39] and pincer ligands.[40]

In this account, we describe the structure and spectroscopic properties of complexes formed by insertion of Ni, Pd, Zn, Cd, and Fe ions into 22-acetoxy-*m*-benziporphyrin or 22-hydroxy-*m*-benziporphyrin. In the case of paramagnetic systems, the relation between paramagnetic shifts and the molecular structure will be discussed in detail.

Results and Discussion

Formation and Characterization of 22-Hydroxy-6,11,-16,21-tetraphenyl-*m*-benziporphyrin (5). Complexes of (TPBPOH)H have usually been obtained directly from acetoxybenziporphyrin, which is a readily available derivative of *m*-benziporphyrin.[7] Metal insertion and acetyl removal are combined in these reactions, making the preparation of **5** unnecessary. Hydroxybenziporphyrin has been prepared, however, to investigate its own reactivity toward metal ions, especially those that do not induce ester cleavage in acetoxybenziporphyrin (Zn(II), Cd(II)).

Compound **5** has been obtained as the dichloride salt by refluxing a chloroform solution of **4** with concentrated hydrochloric acid for 2 h and subsequent precipitation with *n*-hexane. Electronic and ^{1}H NMR spectra of $[\mathbf{5}-H_2]Cl_2$ are shown in Figures 1 and 2, respectively. They are similar to the corresponding spectra obtained for the protonated *m*-benziporphyrin, reflecting similarities in the electronic and molecular structure. In the ^{1}H NMR spectrum, the resonances of exchangeable protons 22-OH, 23,25-NH, and 24-NH have been identified at 9.43, 12.12, and 8.04 ppm (CD_2Cl_2, 233 K). The latter two signals show four-bond scalar couplings to the corresponding β-pyrrole resonances ($^4J_{HH} \approx 1$ Hz). Proton 22-OH could be assigned using the correlations to 22-C and 1,5-C found in the heteronuclear multiple-bond correlation (HMBC) map.

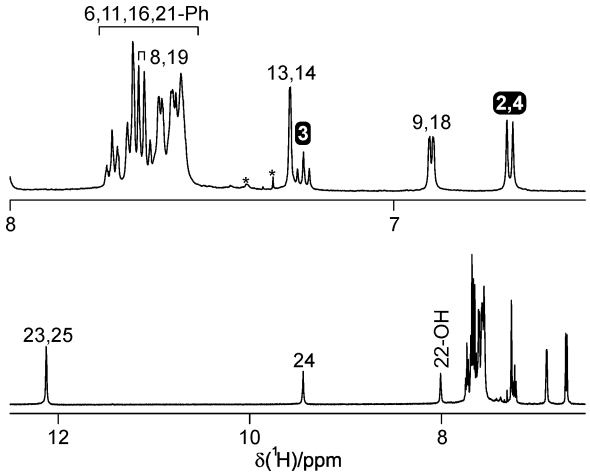

Figure 2. ^{1}H NMR spectrum of $[\mathbf{5}-H_2]Cl_2$ (CD_2Cl_2, 233 K). The high-field region is expanded in the upper trace.

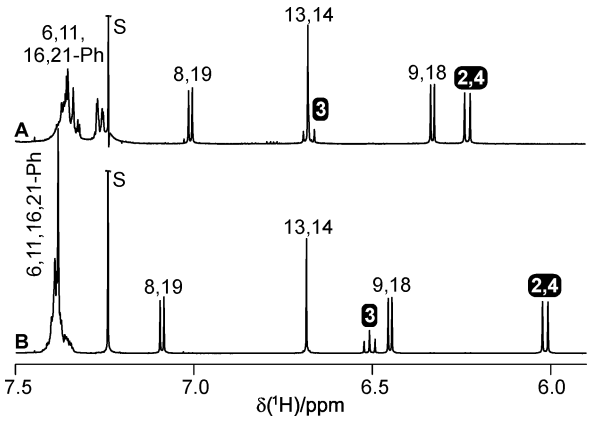

Figure 3. ^{1}H NMR spectra ($CDCl_3$, 298 K) of **6**−Ni (trace A) and **6**−Pd (trace B).

Scheme 3

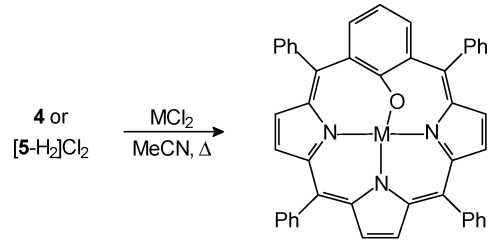

6-M (M = Ni, Pd)

The dicationic form is stable, providing that it is protected from loss of HCl. Deprotonation in solution results in complex equlibria, which are currently under investigation.

Formation and Characterization of (TPBPO)Ni^{II} and (TPBPO)Pd^{II}. Insertion of nickel(II) chloride to **4** in acetonitrile results in the formation of a four-coordinate diamagnetic complex, (TPBPO)Ni^{II} (**6**−Ni) in 74% yield (Scheme 3). The same complex was obtained by reacting $[\mathbf{5}-H_2]Cl_2$ with $NiCl_2$. The palladium species (TPBPO)Pd^{II} (**6**−Pd) was obtained analogously.

The ^{1}H NMR spectra of **6**−Ni and **6**−Pd are presented in Figure 3. NMR data are consistent with the formation of four-coordinate complexes. The ^{1}H and ^{13}C resonances corresponding to the CH_3 and CO fragments of the free

(39) Olmstead, M. M.; Sigel, G.; Hope, H.; Xu, X.; Power, P. P. *J. Am. Chem. Soc.* **1985**, *107*, 8087.
(40) van der Boom, M. E.; Liou, S.-Y.; Ben-David, Y.; Shimon, L. J. W.; Milstein, D. *J. Am. Chem. Soc.* **1998**, *120*, 6531.

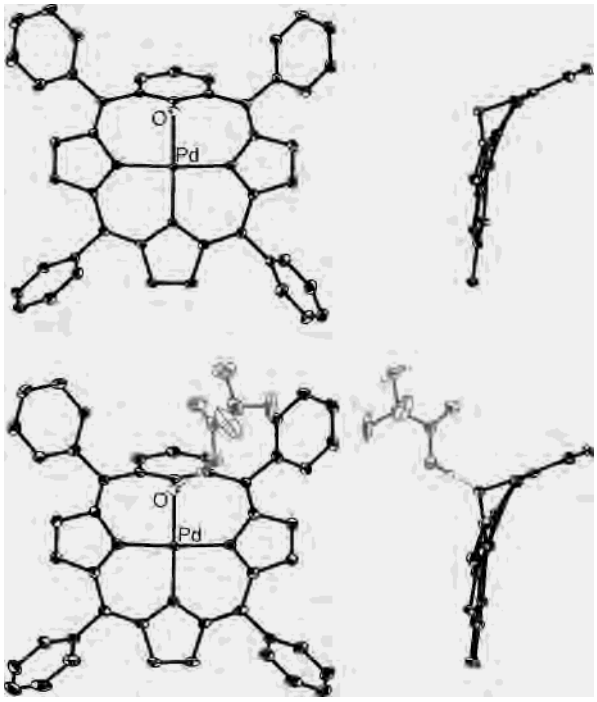

Figure 4. Crystal structure diagrams of **6**−Pd·$CDCl_3$ (top) and **6**−Pd·TFA·$2CDCl_3$ (bottom). Thermal ellipsoids are at the 50% probability level. N atoms are shaded in gray and O atoms in black. H atoms and solvent molecules are omitted for clarity. Phenyl substituents are not shown in the side views. The TFA molecule is drawn in gray lines.

acetoxybenziporphyrin (**4**) are missing in the respective spectra, confirming the absence of the acetyl group.

Crystal Structure of (TPBPO)Pd^{II}. The structure of **6**−Pd, determined in an X-ray diffraction study, is shown in Figure 4 (top). The coordination environment of the Pd ion is roughly square planar and is constituted by three pyrrolic donors and one phenoxide donor. The Pd−N distances are in the limits found for palladium(II) porphyrins,[41] although the Pd−N(24) bond length of 1.981(2) Å is noticeably smaller than the remaining two (2.013(2) and 2.010(2) Å). The Pd−O bond length of 1.992(1) Å is similar to that determined in a palladium(II) phenoxy pincer ligand complex (2.041(2) Å)[40] and comparable to the distance found in the palladium(II) complexes of a substituted salicylaldimine (1.982(4) Å).[42] The C(22)−O distance (1.326(2) Å) is typical of phenoxide ligands.

The coordination square is slightly ruffled with angles N(24)−Pd−O(22) and N(23)−Pd−(N25) equal to 167.1(1) and 175.2(1)°, respectively. The cis X−Pd−Y angles (X, Y = N, O) fall in the range of 87−92°. The Pd atom lies 0.08 Å away from the mean N_3O plane, which is less than the mean deviation of the four donor atoms (0.14 Å).

Introduction of the additional oxygen into the coordination core causes strain, which is partly relieved by bending the phenolate moiety out of the macrocyclic plane (the phenolate itself remains planar). The dihedral angle between the plane of the phenolate (C_6O) and that of the three nitrogens (N_3) is 62.1°. The 6,21 meso carbons are displaced from the N_3 plane in the direction opposite to the oxygen atom, but the remaining part of the macrocycle is only slightly ruffled. Similar conformation was observed in the nickel(II) complexes of the octaethylporphyrin-*N*-oxide dianion,[30] where the oxygen was inserted between the nickel ion and one of the porphyrin nitrogens.

The strain is most noticeable in the C(22)−O−Pd bond angle, which is contracted to 99.6(1)°. A similar geometry, with the C_{ipso}−O−Pd angle of 98.85(14)° was found in the palladium pincer phenoxide of Milstein et al.[40] On the other hand, in the Pd(II) complex of a substituted salicylaldimine,[42] where no strain is present, the pertinent angle is 127.4(3)°. Similar values are observed for other metal phenoxides where no restraint is imposed by the ligand structure.[39,43−45]

As a result of the strain, the Pd···C(22) distance is only 2.571(2) Å, significantly less than the sum of van der Waals radii (1.63 Å for Pd and 1.77 Å for C).[46] It is, however, still larger than that normally observed for Pd−C bond lengths. The environment of C(22) is planar despite the proximity of the Pd ion, suggesting that the Pd···C(22) interaction has little if any bonding character.

When (TPBPO)Pd^{II} was crystallized in the presence of trifluoroacetic acid, another crystal form was obtained containing the adduct (TPBPO)Pd^{II} TFA. In the X-ray structure (Figure 4, bottom), a molecule of TFA associates to the phenolic oxygen of **6**−Pd via a hydrogen bond (1.51 Å), which forms an angle of ca. 37° with the molecular symmetry plane of **6**−Pd. Formation of the H-bond does not influence significantly the structural parameters of the (TPBPO)Pd^{II} molecule. The structure of the acid adduct shows that (TPBPO)Pd^{II} is not protonated by TFA in the solid state, implying low basicity of the Pd-coordinated phenolate.

Paramagnetic Ni(II) Complexes. When a solution of (TPBPO)Ni^{II} (**6**−Ni) is treated with gaseous hydrogen chloride, a new species is formed that can be formulated as (TPBPOH)Ni^{II}Cl (**7**−Ni, Scheme 4). A similar process can be carried out with acetyl chloride yielding (TPBPOAc)Ni^{II}-Cl (**8**−Ni). Interestingly, no reaction is observed with acetic acid or acetic anhydride. The reactions are reversed by refluxing the products in chloroform. (TPBPOH)Ni^{II}Cl and (TPBPOAc)Ni^{II}Cl are, however, hydrolytically unstable and in the presence of excess HCl or AcCl slowly decompose to the respective free ligands.

Both (TPBPOH)Ni^{II}Cl and (TPBPOAc)Ni^{II}Cl are paramagnetic. The ^{1}H NMR spectrum of the latter compound is presented in Figure 5A. It resembles the spectra observed for other high-spin Ni(II) complexes of core-modified porphyrins.[1] The pyrrolic β-H resonances and the 2,4-H signal are shifted to low field, while 3-H and the acetoxy methyl group have their resonances in the upfield region.

(41) Stolzenberg, A. M.; Schussel, L.; Summers, J. S.; Foxman, B. M.; Petersen, J. L. *Inorg. Chem.* **1992**, *31*, 1678.
(42) Miller, K. J.; Baag, J. H.; Abu-Omar, M. M. *Inorg. Chem.* **1999**, *38*, 4510.
(43) Balch, A. L.; Latos-Grażyński, L.; Noll, B. C.; Olmstead, M. M.; Zovinka, E. P. *Inorg. Chem.* **1992**, *31*, 1148.
(44) Darensbourg, D. J.; Widelson, J. R.; Lewis, S. J.; Yarbrough, J. C. *J. Am. Chem. Soc.* **2002**, *124*, 7075.
(45) Redshaw, C.; Elsegood, M. R. J. *Inorg. Chem.* **2000**, *39*, 5164.
(46) Bondi, A. *J. Phys. Chem.* **1964**, *68*, 441.

Scheme 4

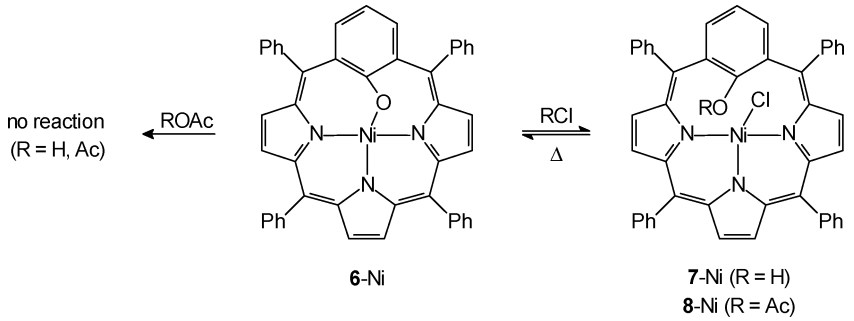

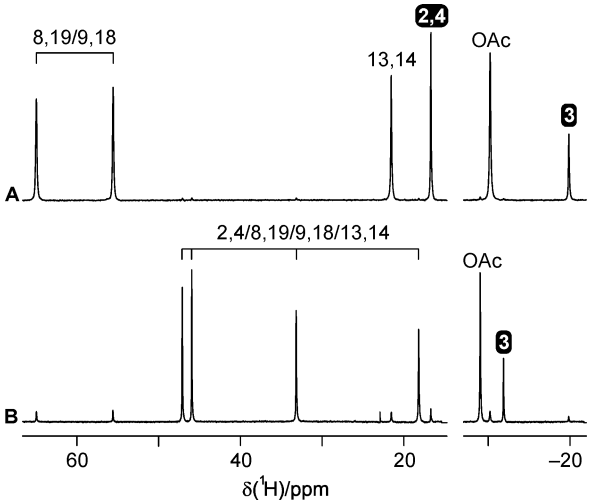

Figure 5. ^{1}H NMR spectrum of **8**−Ni (trace A, 298 K, $CDCl_3$). The diamagnetic region is not shown. Trace B shows the ^{1}H NMR spectrum of the intermediates forming during Ni(II) insertion to **4**. Concentration ratio of the two species is 8.9:1.

To check if any of the two paramagnetic species is an intermediate in the Ni(II) insertion to acetoxybenziporphyrin, the reaction was stopped after a 5 min reflux and worked up in the usual way (see Experimental Section), except for the crystallization step. The ^{1}H NMR spectrum of the product mixture is shown in Figure 5 (trace B, the diamagnetic region, where the signals of (TPBPO)Ni^{II} were present, is not shown). Two paramagnetic species are present, one of which can be identified as (TPBPOAc)Ni^{II}Cl (**8**−Ni) based on the chemical shifts. The spectral pattern observed for the other, more abundant species does not match (TPBPOH)-Ni^{II}Cl, which has similar shift values as (TPBPOAc)Ni^{II}Cl. The new species, which could not be generated from the diamagnetic **6**−Ni, is probably a nickel(II) acetoxybenzipo-rhyrin with unspecified axial ligation. The ligands that should be taken into acount are the chloride originating from the metal carrier, the acetate released during insertion, and acetonitrile.

Other Diamagnetic Metal Ions. Zinc(II) and cadmium-(II) are readily inserted into 22-acetoxy-*m*-benziporphyrin, yielding exclusively the four-coordinate complexes (TPB-POAc)Zn^{II}Cl (**8**−Zn) and (TPBPOAc)Cd^{II}Cl (**8**−Cd), analogous to the previously described (TPBPOAc)Ni^{II}Cl (**8**−Ni). The ester group is not cleaved during the insertion of Zn and Cd even after prolonged reflux of the acetonitrile solutions. The cleavage observed for Ni(II) and Pd(II)

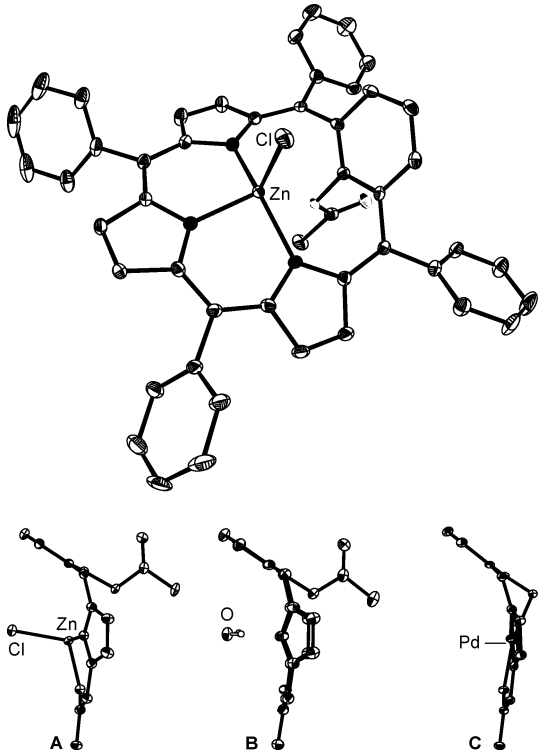

Figure 6. Crystal structure diagram of **8**−Zn·$2CD_2Cl_2$ with thermal ellipsoids at the 50% probability level. Hydrogen atoms and solvent molecules are omitted for clarity. The bottom part of the figure compares the solid-state conformations of **8**−Zn (A), **4** (B, with a hydrogen bonded water molecule), and **6**−Pd (C).

insertions (resulting in **6**−Ni and **6**−Pd) is probably caused by a greater electrophilicity of the d^8 ions accompanied by their tendency to form tetracoordinate planar complexes.

It is possible to generate (TPBPO)Zn^{II} (**6**−Zn) starting from the 22-hydroxybenziporphyrin dication. An unstable compound with a spectrum similar to **6**−Ni and **6**−Pd could be observed in the ^{1}H NMR spectrum of product mixture but was not isolated in pure form.

Crystal Structure of (TPBPOAc)Zn^{II}Cl. The structure of (TPBPOAc)Zn^{II}Cl, determined in an X-ray diffraction study, is shown in Figure 6. In the crystal, the molecule of **8**−Zn is located on a crystallographic symmetry plane (*m*) accompanied by two dichloromethane molecules, one of which is disordered. The acetoxy methyl group shows rotational disorder and was refined in two equally populated orientations. Conformation of the macrocycle closely resembles that of the water adduct of acetoxy-*m*-benziporphyrin[7] (Figure 6).

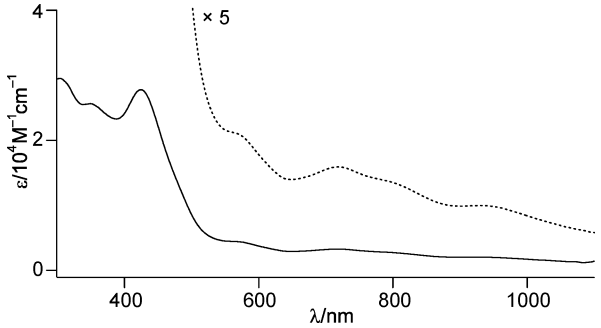

Figure 7. Electronic spectrum of **9**−I (CH_2Cl_2, 298 K).

Scheme 5

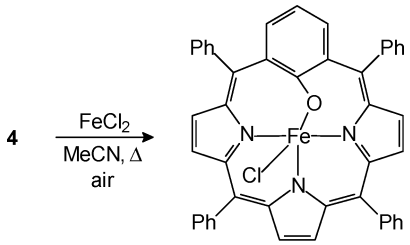

9-Cl

The acetoxy group lies on the side opposite to the chloride. The geometry around zinc can be described as a trigonal bipyramid with the equatorial positions occupied by N(24), the chloride, and the acetoxy-substituted phenylene ring. The coordination bond lengths Zn−N(23), 2.080(3) Å; Zn−N(24), 1.969(5) Å; Zn−N(25), 2.081(3) Å; and Zn−Cl, 2.261(1) Å are in the limits found for the zinc(II) porphyrins and *N*-methyl porphyrins.[47,48] The Zn···C(22) and Zn···O(22) distances (2.794(6) and 2.748(4) Å, respectively) are smaller than the corresponding sums of van der Waals radii (ca. 1.39 Å for Zn, 1.52 Å for O, and 1.77 Å for the benzene ring),[46] indicating a weak, closed-shell interaction. The zinc ion is located 0.58 Å away from the N_3 plane.

Iron Complexes. Insertion of iron into acetoxy-*m*-benziporphyrin (**4**) has been carried out by refluxing the ligand and excess $FeCl_2$ in a chloroform−acetonitrile solution in the presence of atmospheric oxygen. The reaction results yield a five-coordinate complex, (TPBPO)Fe^{III}Cl (**9**−Cl, Scheme 5).

Presumably an iron(II) species (TPBPOAc)Fe^{II}Cl is initially formed. Subsequently acetoxyl cleavage takes place, similarly as during the insertion of Ni(II) and Pd(II), accompanied by aerial oxidation of iron(II). No attempt was made to detect the Fe(II) intermediates in the reaction mixture.

Axial ligand exchange in (TPBPO)Fe^{III}Cl (**9**−Cl) was accomplished by stirring a solution of the complex with hydrobromic or hydriodic acid (see Experimental Section). In this way, the bromoiron and iodoiron complexes (**9**−Br and **9**−I) were obtained. The electronic spectrum of **9**−I is shown in Figure 7.

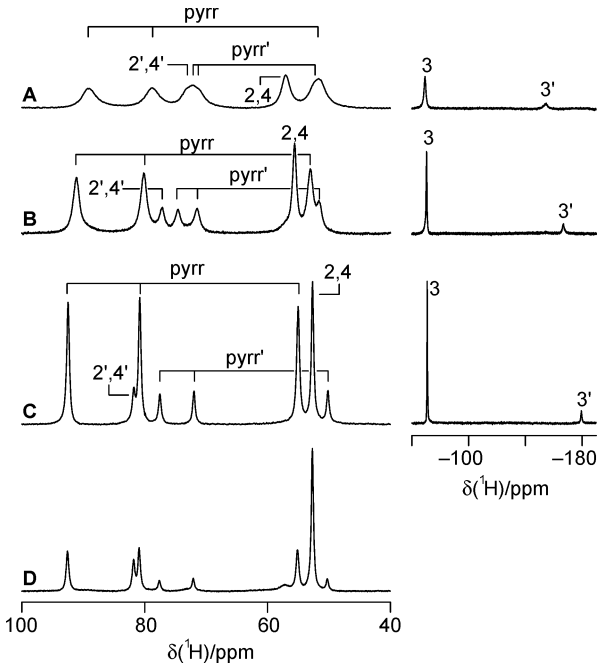

Figure 8. ^{1}H NMR spectra ($CDCl_3$, 323 K) of **9**−Cl (trace A), **9**−Br (trace B), **9**−I (trace C), and **9**−I-d_6 (trace D). The high- and low-field part of each spectrum are not to scale.

The molecule of (TPBPO)Fe^{III}X has an effective C_s symmetry, with the mirror plane passing through the iron atom, chloride, and phenol oxygen. As a consequence, the ^{1}H NMR spectrum will contain three pyrrole resonances (8,-19-H, 9,18-H, and 13,14-H) and two phenol resonances (2,4-H and 3-H, intensity ratio 2:1). Nonequivalence of the two sides of the macrocycle will cause each phenyl ring to have two distinct ortho and two meta resonances, unless the rotation around the $C_{meso}-C_{ipso}$ bond is sufficiently fast.[49]

The ^{1}H NMR spectra of the paramagnetic (TPBPO)Fe^{III}X (X = Cl, Br, I) are shown in Figure 8. Resonance assignments have been made on the basis of relative intensities and site specific deuteration. The ^{1}H NMR spectrum of pyrrole-deuterated (TPBPO-d_6)Fe^{III}I is shown in Figure 8, trace D.

Each of the compounds **9**−X (X = Cl, Br, I) is actually a mixture of two isomers. They will be denoted **9a**−X and **9b**−X, isomer **9b** being the more abundant. Relative amounts of the two isomers were in each case estimated by careful deconvolution of the downfield region of the spectrum, and the results are given in Table 1. The concentration ratios [**9b**−X]/[**9a**−X] determined at 323 K vary from about 2:1 for the chloride (**9**−Cl) to 4:1 for the iodide (**9**−I). The error of these estimations may exceed 10%. Apparently, the composition of the iodide species exhibits certain temperature dependence varying from 6.6:1 at 213 K to 3.9:1 at 323 K (Figure 9), indicating that the two isomers are actually in dynamic equilibrium. Approximate thermodynamic parameters derived from these data are $\Delta H° = -2.6(1)$ kJ/mol and $\Delta S° = 3.7(4)$ J/(mol K) ($r^2 = 0.97$).

(47) Lavallee, D. K.; Kopelove, A. B.; Anderson, O. P. *J. Am. Chem. Soc.* **1978**, *100*, 3025.
(48) Kuila, D.; Lavallee, D. K.; Schauer, C. K.; Anderson, O. P. *J. Am. Chem. Soc.* **1984**, *106*, 448.
(49) Walker, F. A. Proton NMR and EPR Spectroscopy of Paramagnetic Metalloporphyrins. *The Porphyrin Handbook*; Kadish, K. M., Smith, K. M., Guilard, R., Eds.; Academic Press: San Diego, CA, 2000; Vol. 5, Chapter 36, pp 81−183.

Table 1. ^{1}H NMR Chemical Shifts and Line Widths for Complexes **9**−X, X = Cl, Br, I

compound	(TPBPO)Fe^{III}Cl (**9**−Cl)	(TPBPO)Fe^{III}Br (**9**−Br)	(TPBPO)Fe^{III}I (**9**−I)
	Major Isomer (**9b**) δ/ppm ($\nu_{1/2}$/kHz)		
pyrroles	89 (1.4)	91 (0.59)	92 (0.25)
	79 (1.5)	80 (0.61)	81 (0.24)
	∼51 (1.1)	53 (0.58)	55 (0.26)
2,4-H	57 (0.9)	56 (0.39)	53 (0.22)
3-H	−69 (0.9)	−70 (0.30)	−71 (0.18)
	Minor Isomer (**9a**) δ/ppm ($\nu_{1/2}$/kHz)		
pyrroles	∼72 (∼1.4)	75 (0.58)	78 (0.26)
	∼71 (∼1.4)	71 (0.55)	72 (0.24)
	∼53 (1.1)	52 (0.47)	50 (0.26)
2,4-H	∼73 (∼1.4)	77 (0.49)	82 (0.27)
3-H	−155 (2.1)	−167 (0.88)	−180 (0.54)
[**9b**]/[**9a**]	2.1	2.7	3.9

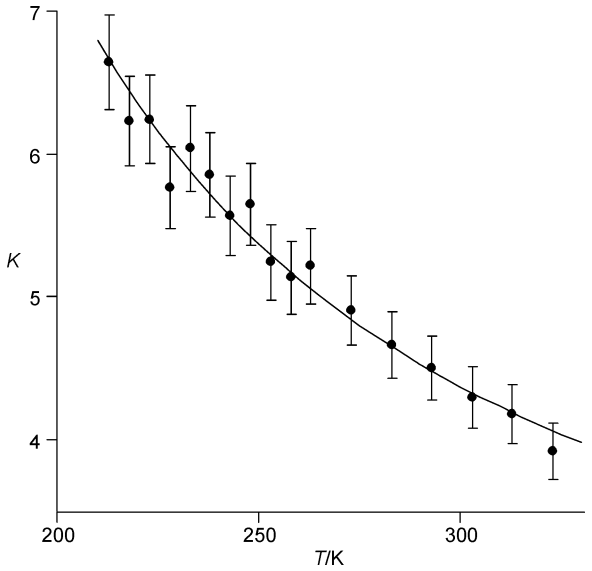

Figure 9. Temperature dependence of the equilibrium constant K = [**9b**−I]/[**9a**−I]. Vertical bars correspond to an error of ±10%. The line shows a least-squares fit of the van't Hoff equation (see text).

Selected chemical shifts and line widths for (TPBPO)-Fe^{III}Cl, (TPBPO)Fe^{III}Br, and (TPBPO)Fe^{III}I are presented in Table 1. The line width increases in the order $I^- < Br^- < Cl^-$, similar to what is observed in high-spin iron complexes of regular porphyrins.[50−53] The signals are therefore best resolved for the iodide complex, which was chosen for detailed spectral analysis.[51,52]

The temperature dependence of the isotropic shifts recorded for the two isomers of (TPBPO)Fe^{III}I (**9**−I) is shown in Figure 10 (the shifts of (TPBPO)Ni^{II} have been taken as the diamagnetic reference). The plots depart visibly from the Curie law, and the curvature results from significant zero-field splitting of the ground electronic state. A satisfactory fit can be obtained, however, by including a term proportional

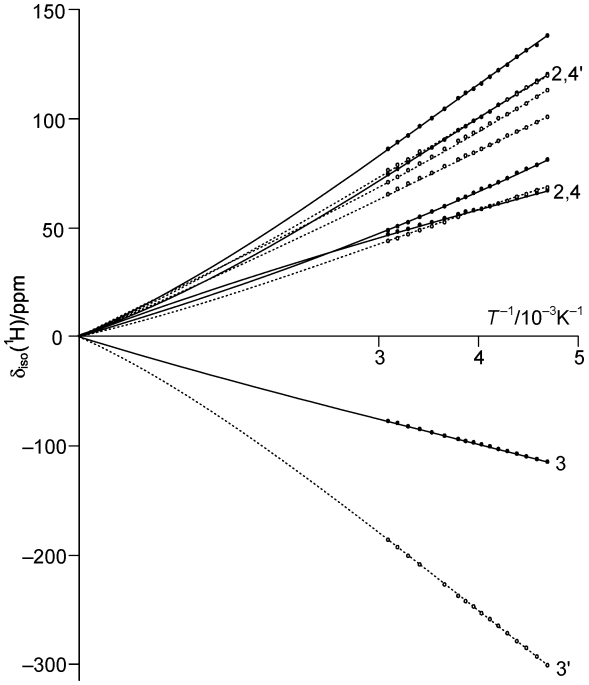

Figure 10. Curie plot for **9**−I (temperature range 213−323 K). Full dots (solid lines) correspond to the major isomer (**9b**−I). Lines are not least-squares fits and are for illustration only. Positive and negative parts of the *Y*-axis are differently scaled.

to T^{-2}, which was shown to correct for the pseudocontact shifts.[51]

Addition of an excess of benzyltriethylammonium chloride to a solution of (TPBPO)Fe^{III}I in $CDCl_3$ results in its conversion to (TPBPO)Fe^{III}Cl, which is characterized by identical isomeric composition to the sample obtained directly from the insertion procedure. In a reverse experiment, the chloride complex **9**−Cl could not be converted into **9**−I even in the presence of a large excess of tetrabutylammonim iodide.

Addition of $AgBF_4$ in CD_3OD to a solution of (TPBPO)-Fe^{III}I transforms the complex into [(TPBPO)Fe^{III}]BF_4, the iodide ligand being removed in the form of AgI. The spectrum of the resulting solution contains only one set of very broad resonances (1−3 kHz, the signal of 3-H was not found). Addition of tetrabutylammonim iodide restores **9**−I, and the ratio of isomers is again exactly reproduced.

Coordination of a metal ion by 22-hydroxybenziporphyrin imposes a steric constraint on the geometry of the ligand. As can be seen in the structure of **6**−Pd, the phenolate moiety is positioned at an angle to the macrocyclic plane. In the ferric complexes **9**−X, the halide ligand can be coordinated on one of the two inequivalent faces of the macrocycle, leading to two distinct species syn and anti, shown in Scheme 6 (the slanted line shows the position of the phenolate).

A similar type of isomerism was previously observed for some chloroiron(III) ocataethylporphyrins substituted in one of the meso positions with AcO,[54] *n*-Bu, OMe, or CHO.[55]

(50) La Mar, G. N.; Walker, A. F. NMR. *The Porphyrins*; Dolphin, D., Ed.; Academic Press: New York, 1979; Vol. IVB, pp 57−161.
(51) La Mar, G. N.; Eaton, G. R.; Holm, R. H.; Walker, F. A. *J. Am. Chem. Soc.* **1973**, *95*, 63.
(52) Balch, A. L.; Cheng, R.-J.; La Mar, G. N.; Latos-Grażyński, L. *Inorg. Chem.* **1985**, *24*, 2651.
(53) Wojaczyński, J.; Latos-Grażyński, L.; Hrycyk, W.; Pacholska, E.; Rachlewicz, K.; Szterenberg, L. *Inorg. Chem.* **1996**, *35*, 6861.
(54) Balch, A. L.; Latos-Grażyński, L.; Noll, B. C.; Olmstead, M. M.; Zovinka, E. P. *Inorg. Chem.* **1992**, *31*, 2248.
(55) Kalish, H.; Camp, J. E.; Stępień, M.; Latos-Grażyński, L.; Olmstead, M. M.; Balch, A. L. *Inorg. Chem.* **2002**, *41*, 989.

Scheme 6

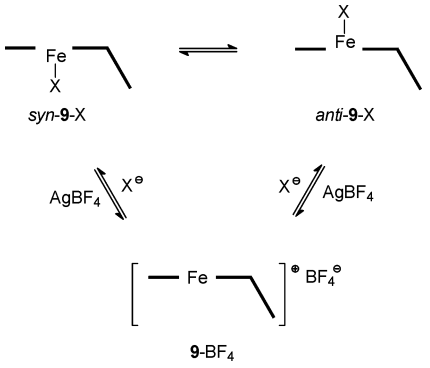

Each of these substituents can be oriented in two different ways (syn or anti) with respect to the axial chloride, and two isomers could be observed by ^{1}H NMR spectroscopy.

Analogous structural diversity is exhibited by complexes of *N*-tosylamido-*meso*-tetraphenylporphyrin. In a recent study it was shown that their stereochemistry depends on the coordinated metal ion.[56] In the gallium(III) species, the axial acetate and the *N*-tosylamide substituent were bound on opposite sides of the macrocycle (the trans isomer), while in the thallium(III) complex they were located on the same side (cis isomer).

Other systems where the discussed kind of isomerism could arise are complexes of *N*-methylporphyrin (N-MeP)H and 21-thiaporphyrin (SP)H, where the presence of the methyl group or the bulky sulfur atom renders the two faces of the macrocycle inequivalent. In a series of (N-MeP)M^{II}-Cl and [(N-MeP)M^{III}Cl]$^+$ complexes, only the anti forms were observed, most probably for steric reasons.[57] Similarly, only the anti isomers formed in the (SP)M^{II}Cl series.[1] Apparently, this steric restriction is not severe and six-coordinate complexes of *N*-methyl- and thiaporphyrins are known where both sides of the macrocycle are occupied with axial ligands.[58] Finally, the trans preference is also demonstrated by the zinc(II) complex of acetoxybenziporphyrin (**6**−Zn).

It is impossible to distinguish the syn and anti forms in the NMR spectra of **9**−X on the basis of chemical shifts alone. Judging by the geometry of the palladium species (**6**−Pd), the two faces of the macrocycle in **9**−X should be similarly accessible to the axial ligand and the preference for one of the isomers may be determined by the overall conformation of the macrocyclic ligand or other, more subtle effects.

When the halide anion is replaced by the noncoordinating BF_4^- to produce **9**−BF_4 (Scheme 6), the source of isomeric differentiation is removed. Coordination of solvent molecules is still possible (MeOH-d_4 used in the experiment) and may yield similar spectroscopic pattern as in the case of **9**−X.

The spectroscopic patterns of the (TPBPO)Fe^{III}X isomers (Figure 8, Table 1) are consistent with their high-spin nature. In all cases (**9**−Cl,Br,I), the downfield shifts of the β-pyrrole signals are greater for the more populated form (**9b**). The isotropic shift values approach those found for high-spin iron(III) tetraarylporphyrins, β-substituted tetraarylporphyrins,[49,53,59] *N*-methylporphyrins,[60,61] and porphycene.[62] The paramagnetic shifts of high-spin iron(III) can be explained by a model typically applied to regular iron porphyrins and iron N-substituted porphyrins. In the case of a high-spin iron(III) center, $(d_{xy})^1(d_{xz}d_{yz})^2(d_{z^2})^1(d_{x^2-y^2})^1$, both σ and π routes of spin-density delocalization operate. The domination of the σ-route results in the downfield shifts of pyrrole resonances observed for (TPBPO)Fe^{III}X.[49,53,59−61,63]

Of particular significance is the shift pattern demonstrated by the phenoxy moiety. Sign alternation of the 2,4- and 3-H resonances is evident for the two isomers (Table 1). Actually, analogous alternation was previously observed for the phenoxide ligand axially coordinated to high-spin iron porphyrins or iron(III) porphycene.[59,62,64−66] The ^{1}H NMR pattern is very characteristic for phenoxide coordination (e.g., (TPP)FeOPh ortho, −118.4; meta, 95; para, −109.7 ppm at 295 K) and was accounted for by π delocalization on the PhO moiety.[59,65] There is a σ donation from the oxygen orbital of axially coordinated phenoxide into the half occupied d_{z^2} orbital of high-spin iron(III). Consequently, it creates a significant amount of spin density on the oxygen orbitals involved in formation of the Fe−O bond. The overlap between oxygen orbitals and the p_z orbital of the ipso carbon provides a route to π spin delocalization onto the phenoxy ligand. An identical mechanism is instrumental in the investigated case of (TPBPO)Fe^{III}I, although, because of the location of the phenoxy group in the meridional plane, the half-occupied $d_{x^2-y^2}$ orbital, instead of d_{z^2}, is included in the discussed delocalization route.

In the three complexes **9**−X (X = Cl, Br, I), the less-populated form is always characterized by a wider spread of the 2,4-H and 3-H resonances. For instance, for the iodide species, the 2,4-H signal of the minor isomer is displaced downfield by 30 ppm compared to the major form. The effect is even stronger for the 3-H resonance, which is shifted upfield by an additional 119 ppm. This indicates that the overlap between the π system of the phenoxy unit and the d orbitals of the iron differs substantially between the two isomers. Arguably, an additional spin delocalization pathway may be operative, resulting from a direct overlap between the d orbitals on the metal center and the π orbitals on the

(56) Tung, J.-Y.; Jiang, J.-I.; Lin, C.-C.; Chen, J.-H.; Hwang, L.-P. *Inorg. Chem.* **2000**, *39*, 1.
(57) Lavallee, D. K. *The Chemistry and Biochemistry of N-Substituted Porphyrins;* VCH Publishers Inc.: New York, 1987.
(58) Latos-Grażyński, L.; Lisowski, J.; Olmstead, M. M.; Balch, A. L. *Inorg. Chem.* **1989**, *28*, 3328.
(59) Arasasingham, R. D.; Balch, A. L.; Hart, R. H.; Latos-Grażyński, L. *J. Am. Chem. Soc.* **1990**, *112*, 7566.
(60) Balch, A. L.; La Mar, G. N.; Latos-Grażyński, L.; Renner, M. W. *Inorg. Chem.* **1985**, *24*, 2432.
(61) Balch, A. L.; Cornman, C. R.; Latos-Grażyński, L.; Olmstead, M. M. *J. Am. Chem. Soc.* **1990**, *112*, 7552.
(62) Rachlewicz, K.; Latos-Grażyński, L.; Vogel, E.; Ciunik, Z.; Jerzykiewicz, L. *Inorg. Chem.* **2002**, *41*, 1979.
(63) Pawlicki, M.; Latos-Grażyński, L. *Inorg. Chem.* **2002**, *41*, 5866.
(64) Godziela, G. M.; Tilotta, D.; Goff, H. M. *Inorg. Chem.* **1986**, *25*, 2142.
(65) Balch, A. L.; Hart, R. H.; Latos-Grażyński, L. *Inorg. Chem.* **1990**, *29*, 3253.
(66) Arasasingham, R. D.; Balch, A. L.; Cornman, C. R.; de Ropp, J. S.; Eguchi, K.; La Mar, G. N. *Inorg. Chem.* **1990**, *29*, 1847.

ipso carbon, C(22). This effect would heavily depend on the Fe···C(22) distance, which presumably differs between the two isomers. As noted before, this distance is small in complex **6**−Pd (2.57 Å).

Conclusion

Two distinct types of metal complexes have been obtained from 22-acetoxybenziporphyrin (**4**). In the species **8**−M (M = Zn, Cd), the acetoxyl substituent is left intact and the metal ion is coordinated to the three nitrogens of the macrocyclic core. In the other group of complexes, exemplified by **6**−M (M = Ni, Pd) and the ferric species **9**−X, the Ac−O bond is cleaved, and the phenolic oxygen participates in binding the metal ion. In the latter case, acetoxybenziporphyrin offers a convenient shortcut to complexes of 22-hydroxybenziporphyrin, making prior hydrolysis of the ester bond unnecessary.

The type of complex that is obtained depends on the metal ion, namely, on its ability to break the ester bond. For instance, (TPBPO)Zn^{II} (**6**−Zn) cannot be synthesized directly from acetoxybenziporphyrin, and [**5**−H_2]Cl_2 has to be used as the ligand source. Conversely, Ni(II) insertion to acetoxybenziporphyrin quickly yields (TPBPO)Ni^{II} (**6**−Ni), and (TPBPOAc)Ni^{II}Cl (**8**−Ni) is observed only as a transient species. **8**−Ni can be synthesized in a reaction of **6**−Ni with acetyl chloride.

The nonplanarity of the macrocycle in the complexes (TPBPO)Fe^{III}X (**9**−X) gives rise to a type of positional isomerism. Ligand X and the deflected *m*-phenylene ring may lie on the same side of the macrocycle or on the opposite sides, leading to two distinct species (syn and anti, respectively).

In complexes **6**−M and **9**−X, the M−O−C angle lies in a plane perpendicular to the phenoxide moiety. This unusual arrangement is a consequence of restraints imposed by the ligand structure, which lead to significant compression of the M−O−C angle.

Further investigations of the hydroxybenziporphyrin complexes may afford an insight into the redox properties of phenols in the presence of metal ions. The macrocyclic structure of the ligand may be expected to stabilize intermediates as well as the frequently elusive products of such reactivity.

Experimental Section

Dichloromethane and acetonitrile were distilled from calcium hydride prior to use. Nickel(II) chloride was dried at 120 °C until yellow. Dilute hydriodic acid was treated with small portions of solid $NaBH_4$ until the disappearance of dissolved iodine.

6,11,16,21-Tetraphenyl-22-acetoxy-*m*-benziporphyrin (**4**) was obtained as previously described.[7]

6,11,16,21-Tetraphenyl-22-hydroxy-*m*-benziporphyrin Dication Dichloride, [5−H_2]Cl_2. Acetoxybenziporphyrin (**4**, 23.5 mg) is dissolved in chloroform (10 mL) and refluxed with concentrated hydrochloric acid (10 mL) for 2 h. Afterward, the organic layer is withdrawn with a pipet, washed once with water, dried with anhydrous calcium chloride, and filtered. The solution is concentrated and the dication precipitated with *n*-hexane. The compound slowly loses HCl upon standing. Yield: 18.0 mg (73%). ^{1}H NMR (CD_2Cl_2, 233 K): 7.8−7.5 (m, 10H, 6,11,16,21-Ph); 12.12, 7.61, 6.90 (ABC: 23,25-H, 8,19-H, 9,18-H, $^3J_{BC}$ = 5.0 Hz, $^4J_{AB} \approx {}^4J_{AC} \approx$ 1 Hz); 9.43 (s, 1H, 22-OH); 8.04, 7.27 (AB_2: 24-H, 13,14-H, $^4J_{AB} \approx$ 1 Hz); 7.24, 6.69 (AB_2: 3-H, 2,4-H, $^3J_{AB}$ = 7.6 Hz). ^{13}C NMR (CD_2Cl_2, 233 K): 158.6 (10,17-C); 150.8 (12,15-C); 149.1 (6,21-Ph); 144.5 (7,20-C); 140.1 (ipso-Ph); 138.0 (2,4-C); 137.6 (8,19-C); 136.8 (ipso-Ph, no correlations found); 135.8 (*o*/*m*-Ph); 133.9 (*o*/*m*/*p*-Ph); 133.3 (*o*/*m*/*p*-Ph); 133.3 (13,14-C); 131.9 (*m*-Ph); 130.5 (1,5-C); 129.6 (*o*/*m*/*p*-Ph); 128.4 (*o*/*m*-Ph); 128.2 (*o*/*m*-Ph); 128.1 (9,18-C); 127.0 (3-C); 115.5 (11,16-C); 113.3 (22-C). UV−vis (CH_2Cl_2, λ_{max} [nm] (log ϵ)): 327 (4.52); 388 (4.43); 471 (5.07); 920 (4.09, broad). HRMS (ESI, *m*/*z*): 642.2559 (642.2540 for $C_{46}H_{32}N_3O^+$).

Chlorozinc(II) 6,11,16,21-Tetraphenyl-22-acetoxy-*m*-benziporphyrin (8−Zn). Acetoxybenziporphyrin (**4**, 20 mg) and anhydrous zinc(II) chloride (molar excess) are added to acetonitrile (15 mL) and refluxed under nitrogen for 15 min. The color of the solution changes from blue-green to yellow-brown. The reaction mixture is then cooled and diluted with water (the solution becomes green). The compound is extracted with dichloromethane, and the extracts are dried with anhydrous sodium sulfate and evaporated to dryness. The residue contains practically pure chlorozinc complex. ^{1}H NMR ($CDCl_3$, 298 K): 7.65−7.60, 7.54−7.43 (m, 10H, 6,11,16,21-Ph); 7.54, 6.86 (AB: 8,19-H, 9,18-H, $^3J_{AB}$ = 5.1 Hz); 7.41, 7.15 (AB_2: 3-H, 2,4-H, $^3J_{AB}$ = 7.7 Hz); 7.13 (s, 2H, 13,14-H); 1.14 (s, 3H, Me). ^{13}C NMR ($CDCl_3$, 298 K): 168.1 (CO); 168.0 (10,17-C); 160.6 (12,15-C); 152.9 (7,20-C); 141.6 (6,21-ipso-Ph); 139.7 (11,16-ipso-Ph); 137.3 (6,21-C); 135.4 (8,19-C); 134.3 (13,14-C); 134.1 (*o*-Ph); 133.3 (1,5-C); 132.7 (*o*/*m*-Ph); 131.9 (9,-18-C); 131.6 (2,4-C); 129.5 (3-C); 129.0 (*o*/*m*/*p*-Ph); 127.8, 127.7, 127.6 (*o*/*m*/*p*-Ph); 116.8 (11,16-C); 102.8 (22-C); 20.1 (Me). UV−vis (CH_2Cl_2, λ_{max} [nm] (log ϵ)): 428 (4.92); 567 (3.39); 820 (4.48). HRMS (ESI, *m*/*z*): 746.1798 (746.1780 for $C_{48}H_{32}N_3O_2Zn^+$).

Chlorocadmium(II) 6,11,16,21-Tetraphenyl-22-acetoxy-*m*-benziporphyrin (8−Cd). Acetoxybenziporphyrin (**4**, 20 mg) and anhydrous cadmium(II) chloride[67] (molar excess) are added to a mixture of chloroform and acetonitrile (10 + 10 mL) and refluxed under nitrogen for 30 min. The yellow-brown solution is then evaporated to dryness, redissolved in a small volume of dichloromethane, and filtered through a Teflon disk. The solvent is removed and the chlorocadmium complex is obtained quantitatively. ^{1}H NMR ($CDCl_3$, 298 K): 7.62−7.59, 7.53−7.42 (m, 10H, 6,11,-16,21-Ph); 7.50, 6.78 (AB: 8,19-H, 9,18-H, $^3J_{AB}$ = 5.0 Hz); 7.48, 7.26 (AB_2: 3-H, 2,4-H, $^3J_{AB}$ = 7.7 Hz); 7.11 (s, 2H, 13,14-H); 1.26 (s, 3H, Me). ^{13}C NMR ($CDCl_3$, 298 K): 169.0 (10,17-C); 168.8 (CO); 162.8 (12,15-C); 153.0 (7,20-C); 141.3 (ipso-Ph); 140.1 (ipso-Ph); 135.4 (6,21-C); 135.0 (13,14-C); 134.6 (8,19-C); 133.9 (*o*-Ph, may overlap with 1,5-C); 133.3 (9,18-C, may overlap with 1,5-C); 132.8 (*o*/*m*-Ph); 131.9 (2,4-C); 130.7 (3-C); 129.2, 128.0, 127.8, 127.5 (*o*/*m*/*p*-Ph); 117.5 (11,16-C); 102.7 (22-C); 20.1 (Me).

Palladium(II) 6,11,16,21-Tetraphenyl-22-hydroxy-*m*-benziporphyrin (6−Pd). Acetoxybenziporphyrin (**4**, 9.1 mg, 13.3 μmol) and palladium(II) chloride (3.2 mg, 18 μmol) are refluxed in acetonitrile (15 mL) under nitrogen. After 4 h, the reaction mixture is evaporated to dryness, and the product is recrystallized from dichloromethane/hexane. Yield: 6.7 mg (67%). ^{1}H NMR ($CDCl_3$, 298 K): 7.34−7.43 (m, 10H, 6,11,16,21-Ph); 7.09, 6.45 (AB: 8,-19-H, 9,18-H, $^3J_{AB}$ = 5.3 Hz); 6.68 (s, 2H, 13,14-H); 6.51, 6.01 (AB_2: 3-H, 2,4-H, $^3J_{AB}$ = 7.7 Hz). ^{13}C NMR ($CDCl_3$, 298 K): 160.5 (10,17-C); 154.9 (12,15-C); 152.7 (7,20-C); 147.2 (6,21-C);

(67) *Handbook of Preparative Inorganic Chemistry*, 2nd ed.; Bauer, G., Ed.; Acadamic Press: New York, London, 1963.

Table 2. Crystal Structure Data for **6**−Pd, **6**−Pd·TFA, and **8**−Zn

	6−Pd·$CDCl_3$	**6**−Pd·TFA·$2CDCl_3$	**8**−Zn·$2CD_2Cl_2$
cryst grown by	slow evaporation of a $CDCl_3$ solution	slow evaporation of a $CDCl_3$ solution	slow evaporation of a CD_2Cl_2 solution
cryst habit	dark prism	dark prism	dark irregular block, violet luster
formula	$C_{47}H_{29}DCl_3N_3OPd$	$C_{50}H_{29}D_2Cl_6F_3N_3O_3Pd$	$C_{50}H_{32}D_4Cl_5N_3O_2Zn$
fw	865.5	1099.9	957.4
a, Å	15.0961(7)	14.9805(9)	10.0525(5)
b, Å	14.6038(9)	13.8084(7)	17.7456(8)
c, Å	16.7035(9)	22.1604(10)	12.3798(7)
α, °			
β, °	93.027(4)	100.337(5)	102.527(5)
γ, °			
V, Å^3	3677.3(3)	4509.6(4)	2155.83(19)
Z	4	4	2
D_{calc}, g·cm^{-3}	1.563	1.617	1.469
cryst syst	monoclinic	monoclinic	monoclinic
space group	$P2_1/n$	$P2_1/c$	$P2_1/m$
cryst size, mm	0.3 × 0.5 × 0.5	0.2 × 0.2 × 0.4	0.4 × 0.6 × 0.6
μ, mm^{-1}	0.766	0.828	0.925
absorption correction	psi-scan (ellipsoid)	psi-scan (ellipsoid)	psi-scan (ellipsoid)
T_{min}, T_{max}	0.736, 0.843	0.636, 0.707	0.341, 0.402
T, K	100 (2)	100 (2)	100 (2)
θ range	$3.71 \le \theta \le 28.38$	$3.26 \le \theta \le 28.48$	$3.37 \le \theta \le 28.39$
hkl range	$-19 \le h \le 20$	$-19 \le h \le 17$	$-13 \le h \le 13$
	$-19 \le k \le 16$	$-18 \le k \le 18$	$-22 \le k \le 19$
	$-21 \le l \le 21$	$-28 \le l \le 29$	$-16 \le l \le 15$
reflns measd	8543	10560	5146
unique reflns, $I \ge 2\sigma(I)$	7571	8664	4753
parameters/restraints	629/6	667/3	305/0
R1	0.0290	0.0374	0.0649
wR2	0.0686	0.0936	0.1636
S	1.085	1.100	1.324
ρ_{max}/ρ_{min}, e·Å^3	0.55/−1.02	1.21/−0.75	0.67/−0.71

142.5 (ipso-Ph); 139.0 (8,19-C); 138.6 (ipso-Ph);137.6 (2,4-C); 134.1 (13,14-C); 132.9, 132.0, 131.7 (*o*/*m*/*p*-Ph); 131.0 (1,5-C); 128.0, 127.9, 127.6, 126.9 (*o*/*m*/*p*-Ph); 126.7 (22-C); 125.3 (9,18-C); 121.7 (3-C); 115.8 (11,16-C). UV−vis (CH_2Cl_2, λ_{max} [nm] (log ϵ)): 349 (4.41); 396 (4.58); 437 (4.58); 607 (4.11); 873 (3.50). HRMS (ESI, *m*/*z*): 746.1459 (746.1418 for $C_{46}H_{30}N_3O^{106}Pd^+$).

Nickel(II) 6,11,16,21-tetraphenyl-22-hydroxy-*m*-benziporphyrin (**6**−Ni) is prepared analogously to the palladium species using 1 equiv (or slight excess) of anhydrous nickel(II) chloride. Alternatively, [**5**−H_2]Cl_2 (12.4 mg, 17 mmol) is refluxed in MeCN with $NiCl_2$ (5 mg, 38 mmol) for 5 h. The solution is then evaporated, redissolved in CH_2Cl_2, filtered through a Teflon disk, and crystallized from CH_2Cl_2/*n*-hexane to afford the nickel(II) complex **6**−Ni (9 mg, 74%). ^{1}H NMR ($CDCl_3$, 298 K): 7.40−7.24 (m, 10H, 6,-11,16,21-Ph); 7.01, 6.33 (AB: 8,19-H, 9,18-H, $^3J_{AB}$ = 5.3 Hz); 6.68 (s, 2H, 13,14-H); 6.68, 6.23 (AB_2: 3-H, 2,4-H, $^3J_{AB}$ = 7.7 Hz). ^{13}C NMR ($CDCl_3$, 298 K): 163.1 (10,17-C); 156.6 (12,15-C); 155.2 (7,20-C); 144.3 (6,21-C); 142.3 (11,16-ipso-Ph); 140.1 (8,19-C); 138.3 (6,21-ipso-Ph, no correlations found); 137.4 (2,4-C); 134.3 (13,14-C); 133.3 (1,5-C); 132.6 (*o*-Ph); 132.0, 131.5 (broad, *o*/*m*/*p*-Ph); 129.8 (22-C); 127.9, 127.5, 126.8 (*o*/*m*/*p*-Ph); 125.9 (9,18-C); 121.3 (3-C); 115.1 (11,16-C). UV−vis (CH_2Cl_2, λ_{max} [nm] (log ϵ)): 329 (4.44); 368 (4.54); 439 (4.68); 637 (3.61); 890 (3.51). HRMS (ESI, *m*/*z*): 697.1648 (697.1659 for $C_{46}H_{29}N_3ONi^+$).

Chloroiron(III) 6,11,16,21-Tetraphenyl-22-hydroxy-*m*-benziporphyrin (**9**−**Cl**)**.** Acetoxybenziporphyrin (**4**, 15.7 mg, 23 mmol) and anhydrous iron(II) chloride (10 mg, 79 mmol) are refluxed in acetonitrile (25 mL) for 3 h. The reaction mixture is poured into 50 mL of water, and the complex is extracted with dichloromethane. The extracts are dried with anhydrous sodium sulfate and filtered, and the solvent is removed. The residue is crystallized from CH_2Cl_2−MeOH to give the chloroiron(III) species **9**−Cl (13.5 mg, 80%). **HRMS** (ESI, *m*/*z*): 695.1674 (695.1655 for $C_{46}H_{29}N_3OFe^+$).

Iodoiron(III) 6,11,16,21-Tetraphenyl-22-hydroxy-*m*-benziporphyrin (**9**−**I**)**.** The chloroiron(III) complex **9**−Cl is dissolved in a small volume of chloroform and stirred with hydriodic acid (concentrated stock solution diluted with water in 1:10 ratio) for 1 h (progress of the axial ligand exchange was monitored by ^{1}H NMR spectroscopy). UV−vis (CH_2Cl_2, λ_{max} [nm] (log ϵ)): 302 (4.47); 348 (4.41); 424 (4.44); 718 (3.50); 931 (3.30). The bromoiron(III) species (**9**−Br) was obtained analogously using aqueous HBr.

Instrumentation. NMR spectra were recorded on a Bruker Avance 500 spectrometer (base frequencies ^{1}H, 500.13 MHz; ^{13}C, 125.77 MHz) equipped with a broadband inverse gradient probehead, a dual ^{1}H−^{13}C gradient probehead, or a direct broadband probehead. Spectra were referenced to the residual solvent signals. Except for NOESY spectra, all 2D experiments were gradient selected. The DPFGSE experiment was performed using pulse program *selnogp.3* from the standard Bruker library. Gaussian pulses were employed with a duration of 50 ms. Assignments of ^{13}C spectra were obtained from ^{1}H−^{13}C HSQC and HMBC experiments.

X-ray Data Collection and Refinement. Crystals of **6**−Pd, **6**−Pd·TFA, and **8**−Zn were grown by slow evaporation of $CDCl_3$ or CD_2Cl_2 solutions. Crystal data and refinement details are given in Table 2. The data were collected on a Kuma KM4CCD κ-axis diffractometer with graphite-monochromated Mo Kα radiation and processed using the accompanying software. The structures were solved by heavy-atom or direct methods (SHELXS97 [68]) and refined by the full-matrix least-squares method on all F^2 data using the SHELXL97 program.[69] Hydrogen atoms were found in the difference map and refined isotropically (**6**−Pd) or as riding groups (**6**−

(68) Sheldrick, G. M. *SHELXS97 − Program for Crystal Structure Solution.* University of Göttingen: Göttingen, Germany, 1997.
(69) Sheldrick, G. M. *SHELXL97 − Program for Crystal Structure Refinement.* University of Göttingen: Göttingen, Germany, 1997.

Pd·TFA and **8**−Zn). Psi-scan absorption correction was applied.[70] The disordered $CDCl_3$ molecule in **6**−Pd was refined in two orientations with a total unit occupancy. In the remaining structures, the disorder of solvent molecules, as well as that of CH_3 and CF_3 groups, was handled similarly.

Acknowledgment. Financial support from the State Committee for Scientific Research KBN of Poland (Grant 4 T09A 147 22) and the Foundation for Polish Science is kindly acknowledged.

(70) *XPREP Data Preparation and Reciprocal Space Exploration Program.* Bruker Analytical X-ray Systems: 1997.

Supporting Information Available: Crystal data for compounds **6**−Pd, **6**−Pd·TFA, and **8**−Zn are included in CIF format. The material is available free of charge via the Internet at http://pubs.acs.org.

IC0345121